surfaces

MDPI

Article

High-Pressure and High-Temperature Dissolution of Titanium from Titanium and Aluminum Residues: A Comparative Study

Srecko Stopic [1,*], Duško Kostić [1,2], Elif Emil-Kaya [3], Emircan Uysal [4], Sebahattin Gürmen [4], Aleksandar Mitrašinović [5], Mitar Perušić [2] and Bernd Friedrich [1]

1 IME Process Metallurgy and Metal Recycling, RWTH Aachen University, 52056 Aachen, Germany; dkostic@metallurgie.rwth-aachen.de (D.K.); bfriedrich@metallurgie.rwth-aachen.de (B.F.)
2 Faculty of Technology Zvornik, University of East Sarajevo, Karakaj 34A, 75400 Zvornik, Republic of Srpska, Bosnia and Herzegovina; mitar.perusic@tfzv.ues.rs.ba
3 Department of Materials Science and Engineering, Norwegian University of Science and Technology, Høgskoleringen 1, 7034 Trondheim, Norway; elif.e.kaya@ntnu.no
4 Department of Metallurgical and Materials Engineering, Istanbul Technical University, Reşitpaşa, 34485 İstanbul, Türkiye; emircan.uysal@hotmail.com (E.U.); gurmen@itu.edu.tr (S.G.)
5 Institute of Technical Sciences of Serbian Academy of Sciences and Arts, Knez Mihailova 35, 11000 Belgrade, Serbia; aleksandar.mitrasinovic@itn.sanu.ac.rs
* Correspondence: sstopic@metallurgie.rwth-aachen.de; Tel.: +49-17678261674

Abstract: This study presents a comparative analysis of titanium leaching from tionite (a byproduct of the titanium dioxide production process) and carbothermally reduced red mud (derived from aluminum residues). Tionites from the sulfate process and red mud residue are known for their environmental impacts due to their metal content and acidic/basic nature. This study explored leaching as a method to recover titanium and other metals under high-pressure and high-temperature conditions using sulfuric acid. Experiments were conducted in an autoclave with different parameter changes, like varying oxygen pressure, temperature, and reaction time to optimize metal extraction. The leaching efficiency of titanium was found to be higher in the carbothermal-reduced slag compared to tionite due to the altered mineral phases in the reduced material. XRD and SEM-EDS analyses confirmed the differing leaching behaviors, with titanium compounds in tionite showing greater resistance to dissolution. These findings highlight the importance of thermal pre-treatment for optimizing metal recovery from industrial residues. The main aim of this study is to contribute to the development of sustainable waste management solutions for tionites and red mud, emphasizing the potential of hydrometallurgical methods for metal recovery. The results are expected to inform future research and industrial applications, advancing the recovery of valuable metals while reducing the environmental footprint of titanium and aluminum residue disposal.

Keywords: carbothermally reduced red mud; titanium dioxide residue; high-pressure leaching; titanium recovery

Citation: Stopic, S.; Kostić, D.; Emil-Kaya, E.; Uysal, E.; Gürmen, S.; Mitrašinović, A.; Perušić, M.; Friedrich, B. High-Pressure and High-Temperature Dissolution of Titanium from Titanium and Aluminum Residues: A Comparative Study. *Surfaces* **2024**, *7*, 1096–1108. https://doi.org/10.3390/surfaces7040072

Academic Editor: Gaetano Granozzi

Received: 18 September 2024
Revised: 1 December 2024
Accepted: 18 December 2024
Published: 20 December 2024

1. Introduction

Titanium dioxide residues (tionites) are solid residues generated during the production of titanium dioxide (TiO_2) via the chloride and sulfate processes. These residues typically contain unreacted minerals, iron oxides, silicates, and other metal oxides, along with residual titanium compounds. The specific mineralogical composition of tionites can vary depending on the processing method, but they commonly include minerals such as ilmenite ($FeTiO_3$), rutile (TiO_2), and anatase (TiO_2), along with iron oxides such as hematite (Fe_2O_3) and magnetite (Fe_3O_4), as well as silicate minerals like feldspar and quartz. These byproducts are often considered waste, yet they present significant environmental and waste management challenges due to their complex composition and large volume [1–5].

The sulfate process involves the digestion of ilmenite or titanium slag in sulfuric acid to produce titanium oxysulfate, which is then hydrolyzed to form hydrated titanium dioxide. The tionites from this process are more complex, containing iron sulfate ($Fe_2(SO_4)_3$), unreacted ilmenite, and various metal sulfates such as calcium sulfate ($CaSO_4$), magnesium sulfate ($MgSO_4$), and aluminum sulfate ($Al_2(SO_4)_3$). These residues are often acidic, with a high content of sulfate compounds and iron sulfates, and can be more challenging to manage due to their potential to generate a threat to the environment if not properly treated [1,2].

Tionites can have significant environmental impacts if not properly managed. The presence of heavy metals and acid-generating compounds can lead to soil and water contamination. For example, sulfate-process tionites can contribute to the acidification of water bodies and mobilize toxic metals, harming aquatic ecosystems. The chloride-process tionites, while less acidic, can still pose risks due to the presence of heavy metals and other hazardous substances.

To mitigate their environmental impact, researchers and industries are exploring ways to utilize tionites as secondary raw materials. Potential applications include [6–9]:

1. Cement and Construction Materials: Tionites can be used as a raw material in cement production, leveraging their iron and silicate content.
2. Metal Recovery: Residual metals, particularly iron and titanium, can be recovered from tionites through various chemical and physical processes.
3. Soil Amendment: In controlled applications, tionites can be used to neutralize acidic soils, though care must be taken to avoid heavy metal contamination.
4. Landfill Liners: Tionites with low leachability can be used as landfill liners to prevent the spread of contaminants.

The utilization of tionites not only reduces waste but also transforms a potential environmental liability into a valuable resource. However, the feasibility of these applications depends on the specific composition of the tionites, the availability of processing technology, and economic considerations.

Red mud is a byproduct of the Bayer process, which is used to extract alumina (Al_2O_3) from bauxite ore. It is a highly alkaline waste material with a complex composition, including oxides of iron, aluminum, titanium, and various other trace elements. Due to its large volume, strong alkalinity (pH 10–13), and the presence of toxic elements, red mud poses significant environmental challenges. The disposal of red mud is a major concern because it can lead to soil and water contamination, particularly through the leaching of heavy metals and other hazardous substances into surrounding ecosystems [10–12].

Red mud has substantial environmental impacts, including the potential for groundwater pollution, harm to aquatic life, and soil degradation in areas near disposal sites. Accidental spills, such as the one that occurred in Hungary in 2010, can have catastrophic consequences for both the environment and human health. The high alkalinity of red mud makes it corrosive, and managing its disposal requires substantial land area and careful engineering to prevent environmental damage [13,14].

However, red mud also contains valuable elements, such as iron, titanium, and rare earth metals, which have prompted research into its utilization as a secondary resource. Potential uses include its application in the construction industry (e.g., as a component in cement or bricks), as a raw material for the extraction of valuable metals, and in environmental remediation efforts, such as neutralizing acidic soils or wastewater treatment [3,15–17].

In the authors' previous research, the focus was on the carbothermal reduction of red mud, a process that involved heating red mud in the presence of carbon to reduce metal oxides. That method aimed to transform the iron oxides into metallic iron or other more easily leachable forms, thereby improving the potential for metal recovery. The carbothermal reduction was followed by a leaching process, where the reduced red mud was treated with sulfuric acid to extract titanium and other valuable metals.

The current study aims to compare the leaching efficiency of that carbothermally reduced red mud from previous research with that of tionite (sulfate process). By comparing

the leaching behavior of these two materials, the research seeks to optimize the recovery of titanium and other metals while also exploring sustainable methods for managing industrial waste. This approach not only addresses the environmental impact of red mud disposal but also contributes to the circular economy by turning waste into a valuable resource.

Leaching is a critical process in extractive metallurgy used to obtain valuable metals from ores. This technique involves treating the ore with specific chemicals that react with the metal compounds, forming soluble salts while leaving the impurities behind. The soluble salts can then be washed away and further processed to retrieve the pure metal. The remaining material after metal extraction is known as tailings [18].

One major advantage of leaching over pyrometallurgy is its relative ease of operation and the absence of harmful gaseous emissions, which can make it a potentially more environmentally friendly option. While leaching can have lower direct energy requirements compared to some high-temperature pyrometallurgical methods, the total energy consumption for leaching and pyrometallurgy may be comparable in certain processes, depending on the metal and specific conditions [18].

Despite these advantages, leaching has notable drawbacks. It is generally less efficient than pyrometallurgy and produces large volumes of waste effluent and tailings. These waste products are often highly acidic or alkaline and may contain toxic substances, posing significant environmental and health risks [19].

Leaching can be carried out through various methods, including pressure leaching, atmospheric leaching, and ultrasound-assisted leaching. It is often conducted at high temperatures to enhance efficiency. Despite its challenges, leaching is a vital technique in the mining industry, enabling the extraction of metals that might be otherwise economically or technically unfeasible to recover by other methods. Effective management and treatment of leaching effluents and tailings are crucial to minimize environmental impact and ensure the sustainability of this extraction method [20–22].

The novelty of this work lies in its comparative approach to evaluating the high-pressure, high-temperature dissolution of titanium from two distinct industrial residues: tionites (a byproduct of titanium dioxide production) and carbothermally reduced red mud (a byproduct of alumina extraction). This study uniquely combines thermal treatment with subsequent chemical dissolution processes, offering new insights into how the initial treatment conditions influence the recovery efficiency of titanium and other metals. By exploring optimal conditions for titanium recovery from these residues, it contributes to waste valorization and offers sustainable solutions for industrial waste management.

2. Materials and Methods

In this study, Tionite S (sulfate process) from Venator GmbH, along with slag (carbothermally reduced red mud) from the "Alumina" Ltd. factory in Zvornik, Bosnia and Herzegovina , were utilized as raw materials. The tionites and red mud were dried, ground, and prepared for the reduction process. Characterization of these materials was carried out using X-ray diffraction (XRD) and energy-dispersive X-ray spectroscopy (EDS) analyses.

The tionite and slag samples were analyzed at room temperature using X-ray powder diffraction with an Ultima IV Rigaku diffractometer, which employed CuKα1,2 radiation, a generator voltage of 40 kV, and a current of 40 mA. The analysis covered a 2θ range of 10–100° in continuous scan mode, with a step size of 0.02° and a scan rate of 1°/min, utilizing a D/TeX Ultra high-speed detector. A glass sample carrier was used for sample preparation. Phase composition and identification were evaluated with PDXL2 (Ver. 2.8.4.0) software, and all powders were identified using the ICDD database.

Scanning Electron Microscopy (SEM): The surface morphology and microstructural characteristics of the solid samples before and after the leaching experiments were analyzed using a Quattro S scanning electron microscope (Thermo Fisher, Hillsboro, OR, USA). The Quattro S was operated in high vacuum mode with an accelerating voltage of typically 5–20 kV. The images were obtained at various magnifications to observe both the overall particle morphology and finer surface details. Energy-dispersive X-ray spectroscopy (EDS)

was also performed to identify the elemental composition of the sample surfaces, providing insight into the distribution of titanium and other relevant elements across the material matrix. The chemical composition of elements dissolved in the solution was analyzed using high-resolution inductively coupled plasma optical emission spectroscopy (ICP-OES). This technique allows for the detection of elements with atomic mass numbers ranging from lithium (Li) to uranium (U). The analysis was conducted using a Spectro Genesis spectrometer.

Particle size distribution was analyzed using a HELOS (H4011i) laser diffraction system equipped with the RODOS dry dispersion unit (Sympatec GmbH, Clausthal-Zellerfeld, Germany). The HELOS system provides high-resolution measurements across a wide particle size range, utilizing laser diffraction principles. The RODOS dispersion unit ensures efficient deagglomeration of particles through controlled high-velocity air streams, facilitating accurate size distribution analysis. Prior to measurement, samples were dispersed under standardized conditions to achieve consistent reproducibility. Data acquisition and analysis were conducted using the associated WINDOX software 5.7.

Leaching of the slag was performed in a Buchi autoclave from Switzerland, designed specifically for acid leaching (capacity of 1.53 L, max. pressure of 200 bars, and max. temperature of 270 °C). Leaching was carried out using sulfuric acid. This setup includes a heat exchanger with a thermostat, a mixer, pressure adjustment probes, and the capability to extract samples during operation. The autoclave is connected to a computer, allowing for complete control via software that records all operational data for subsequent analysis. The pressure was monitored using both a manometer and digital sensors. The system's pressure comprised oxygen (6–9 bars) and water vapor (total 12–15 bars). Cooling was achieved with a specialized cooling system, and the heating rate was set at 10 °C/min. Prior to each operation, the autoclave was manually sealed with screws and underwent a pressure test to ensure integrity.

The slag, along with Tionite S, was leached under various conditions as detailed in Table 1. Prior to leaching, the slag was ground and sifted.

Table 1. Design of leaching experiments.

Exp. No.	Material	Temperature (°C)	Initial Pressure of O_2 (bar)	Concentration of Acid (mol/dm^3)	Liquid/Solid Ratio (mL/g)	Time (min)
1	Slag	150	0	5	10:1	60
2	Slag	150	6	5	10:1	120
3	Slag	180	6	5	10:1	120
4	Slag	150	9	5	10:1	120
5	Tionite S	150	6	5	10:1	120
6	Tionite S	150	6	5	10:1	60
7	Tionite S	180	6	5	10:1	120
8	Tionite S	150	9	5	10:1	60
9	Tionite S	150	9	5	10:1	120

Leaching these materials, particularly the slag, which primarily contains iron oxide, is a highly complex process with intricate mechanisms. However, the following reactions are typically considered during the leaching process:

$$Fe_2O_{3(s)} + 3\,H_2SO_{4(aq)} \rightarrow Fe_2(SO_4)_{3(aq)} + 3\,H_2O \quad (1)$$

$$TiO_2 + H_2SO_4 \rightarrow [TiO]SO_4 + H_2O \quad (2)$$

$$TiO[SO_4] + \frac{1}{2}O_2 \rightarrow [TiO\text{–}O]SO_4 \quad (3)$$

$$Al_2O_3 + 3\,H_2SO_4 \rightarrow Al_2(SO_4)_3 + H_2O \quad (4)$$

$$CaO + H_2SO_4 \rightarrow CaSO_{4(s)} + H_2O \quad (5)$$

$$CaTiO_3 + H_2SO_4 + 1.5O_2 \rightarrow TiOSO_4 + H_2O + CaSO_4 \quad (6)$$

The design of the leaching experiments is shown in Table 1 and Figure 1.

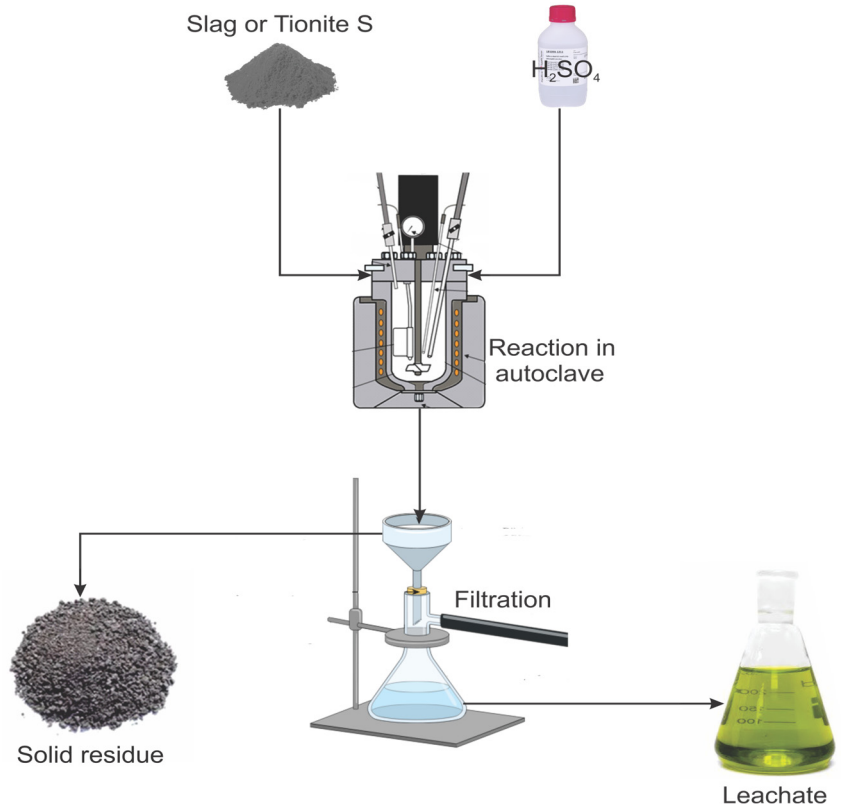

Figure 1. Experimental setup for leaching in an autoclave.

All experiments have been carried out in the laboratories of the IME RWTH.

In this paper, leaching is used to extract titanium from the earlier reduced slag and represents a combination of pyrometallurgical and hydrometallurgical methods of red mud processing in order to optimize and find the optimal processing process. Pure oxygen was needed to react with titanium from slag in order to form a dissolved form of titanium oxysulfate.

3. Results and Discussion

The XRD pattern for tionite from the sulfate process (Figure 2a) primarily shows strong peaks corresponding to rutile (TiO_2), with additional contributions from silica (SiO_2), armalcolite, and minor ilmenite. Rutile dominates the pattern, with silica and armalcolite adding distinct, though weaker, peaks.

For the carbothermally reduced slag (Figure 2b), the XRD pattern is more complex, featuring prominent peaks from $CaTiO_3$, metallic iron, and hematite (Fe_2O_3). Other phases such as magnetite (Fe_3O_4), silica, gehlenite, rutile, and $CaAl_2SiO_6$ contribute to a variety of additional peaks, making this pattern more intricate compared to that of the tionite.

Particle size distribution of slag (Figure 3) shows an increase in particle size due to the reduction in red mud and agglomeration of the particles.

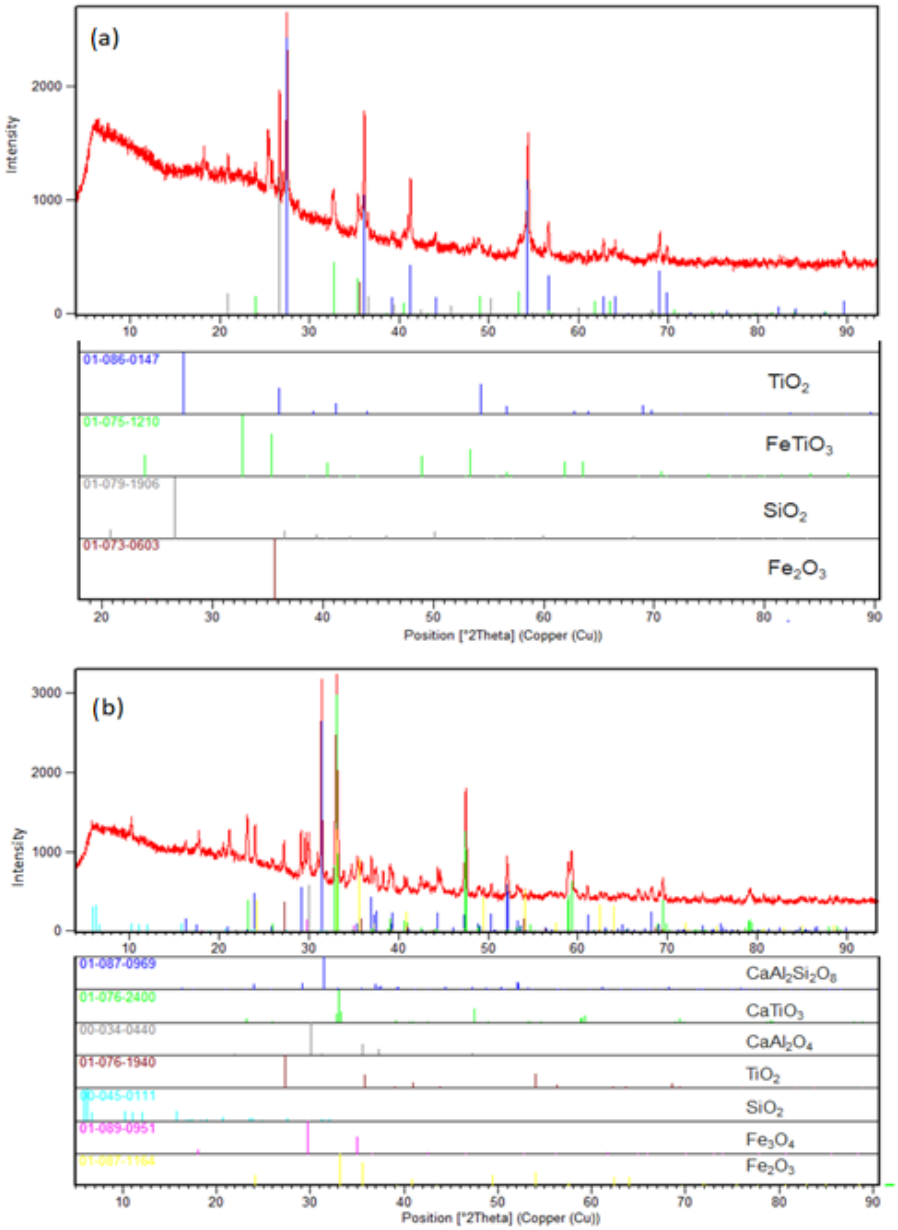

Figure 2. XRD analysis of (**a**) Tionite S and (**b**) carbothermally reduced slag.

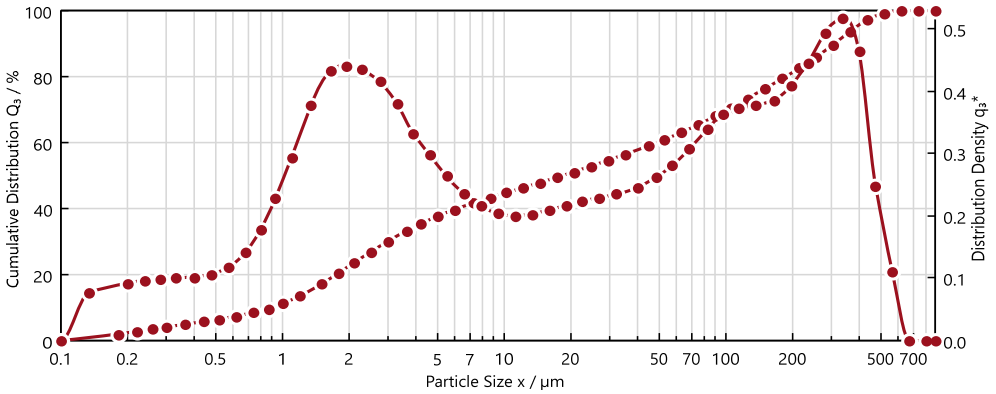

Figure 3. Particle size distribution for slag.

The composition data confirm the XRD analysis (Table 2). Tionite S shows a high titanium content, consistent with the dominance of rutile in the XRD pattern, along with

iron and silicon levels that align with the presence of ilmenite and silica. The slag has lower titanium and iron contents but higher aluminum, reflecting the complex mix of phases like $CaTiO_3$, iron oxides, and aluminosilicates seen in the XRD pattern. Overall, the elemental analysis (EDS) supports the identified mineral phases in both materials.

Table 2. Composition of Tionite S and slag.

Sample	Ti (%)	Fe (%)	Al (%)	Si (%)
Tionite S	29	10.1	1.53	7.63
Slag	5.9	8.2	12.2	6.4

The microstructure of Figure 4a Tionite S reveals a predominantly fine-grained, fragmented morphology with irregularly shaped particles. The smaller particles and their agglomeration suggest a high surface area, which may influence its reactivity during leaching. The overall structure appears brittle and heterogeneous.

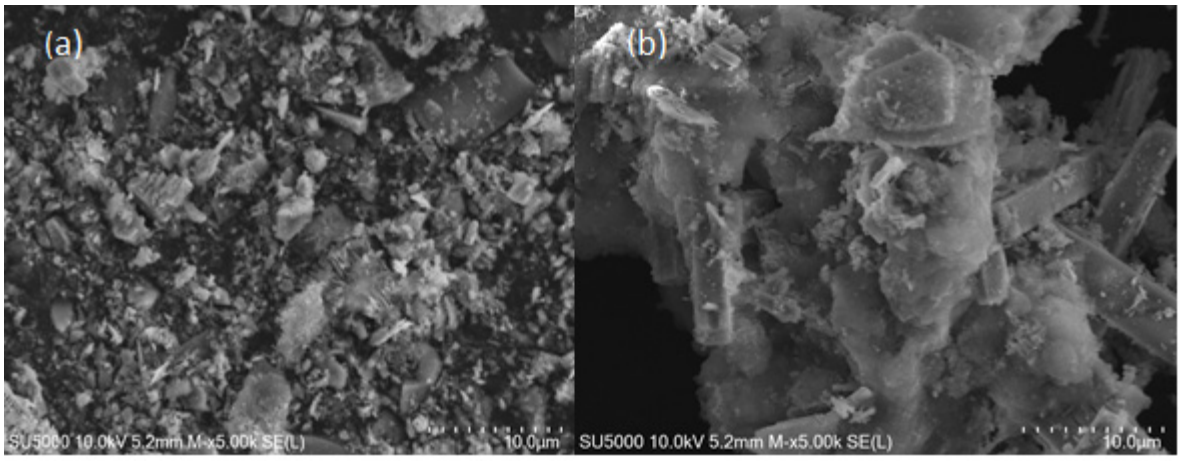

Figure 4. (**a**) SEM image of Tionite S and (**b**) SEM image of slag.

In contrast, Figure 4b Slag displays larger, more consolidated structures with layered and plate-like formations. These features suggest higher thermal stability and a denser composition compared to Tionite S.

Figure 5 presents the leaching efficiencies of iron (Fe), titanium (Ti), and aluminum (Al) from slag using 5 M sulfuric acid under varying conditions of oxygen pressure and temperature. The first experiment showed that leaching of the slag at atmospheric pressure showed low leaching efficiencies of all three elements, particularly titanium. In the second experiment, conducted at 150 °C for 2 h under 6 bars of oxygen pressure, Fe, Ti, and Al were all leached with relatively high efficiencies.

In the third experiment, where the temperature was increased to 180 °C while maintaining the same reaction time and pressure, Fe and Al leaching efficiencies improved significantly. However, Ti leaching efficiency dropped considerably, which might be due to the formation of more stable titanium compounds or a re-precipitation process under the higher temperature, making Ti less soluble.

In the fourth experiment, where the oxygen pressure was increased to 9 bars while keeping the temperature at 150 °C and the reaction time at 2 h, all three metals—Fe, Ti, and Al—achieved near-complete leaching. The higher oxygen pressure likely enhanced the oxidation process, improving the dissolution of these metals, especially Ti, which had the highest leaching efficiency under these conditions. This trend suggests that increased pressure can be a critical factor in maximizing the extraction of metals from slag, particularly for those like Ti that are otherwise more challenging to leach effectively at higher temperatures. Leaching efficiencies were calculated by comparing the concentration of

selected elements in the leachates (performed by ICP-OES) to the total amount of those elements initially present in the solid material before leaching.

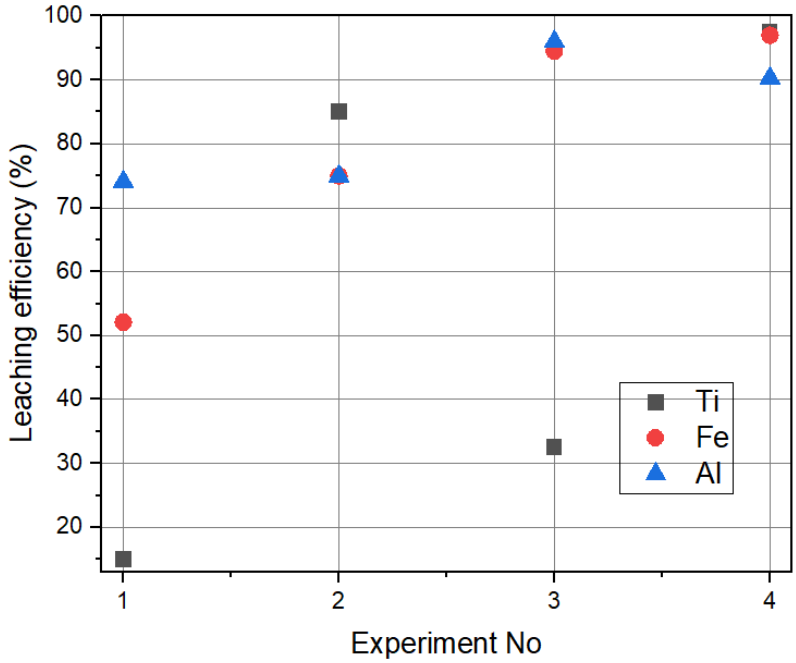

Figure 5. Leaching efficiency of slag under different parameters.

Figure 6 shows the leaching efficiencies of iron (Fe), titanium (Ti), and aluminum (Al) from Tionite S using 5 M sulfuric acid under 6–9 bars of oxygen pressure across three different experiments. In the fifth experiment, conducted at 150 °C for 2 h, Fe was leached efficiently, while Ti and Al showed moderate to low leaching efficiencies. When the reaction time was reduced to 60 min while maintaining the same temperature, Fe and Al leaching efficiencies remained consistent, but Ti leaching increased slightly.

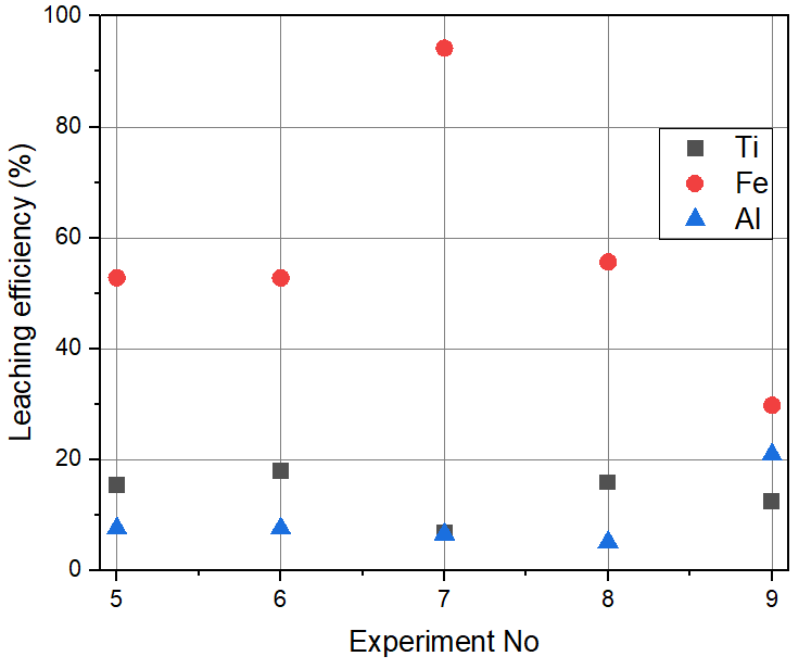

Figure 6. Leaching efficiency of Tionite S under different parameters.

In the seventh experiment, where the temperature was raised to 180 °C and the reaction time was kept at 2 h, there was a notable increase in Fe leaching efficiency. However, Ti and Al leaching efficiencies decreased. The reduced leaching of Ti at the higher temperature could be attributed to the formation of more stable titanium compounds or the re-precipitation of Ti as less soluble species under these conditions, which prevents their dissolution. This suggests that while higher temperatures enhance Fe extraction, they may simultaneously limit the leaching of Ti due to changes in the mineral's chemical behavior.

In the eighth experiment, where oxygen pressure was increased to 9 bars, we observed a decrease in titanium (Ti) leaching compared to the sixth experiment at 6 bars. This suggests that the higher oxygen pressure may have influenced the formation of more stable titanium phases, reducing the efficiency of Ti leaching. On the other hand, the leaching of iron (Fe) slightly increased, likely due to a more pronounced oxidation effect at higher pressure. For aluminum (Al), which exhibited the lowest leaching efficiency across all experiments, the result indicates that aluminum compounds are more resistant to leaching under the given conditions. In the ninth experiment, the reaction time was extended to 120 min under the same 9-bar oxygen pressure, leading to the lowest Fe leaching efficiency observed in all experiments. This could be attributed to the preferential leaching of more reactive components before the reaction time was extended. While Ti leaching also decreased, Al leaching showed a slight increase, indicating that longer exposure times may help in the partial dissolution of aluminum-containing compounds.

These findings suggest that Tionite S may require thermal exposure to alter its composition and structure, potentially enhancing the leaching process. We have emphasized this point in the revised manuscript to provide a clearer understanding of the experimental trends.

In Figure 7, SEM-EDS results for slag are shown.

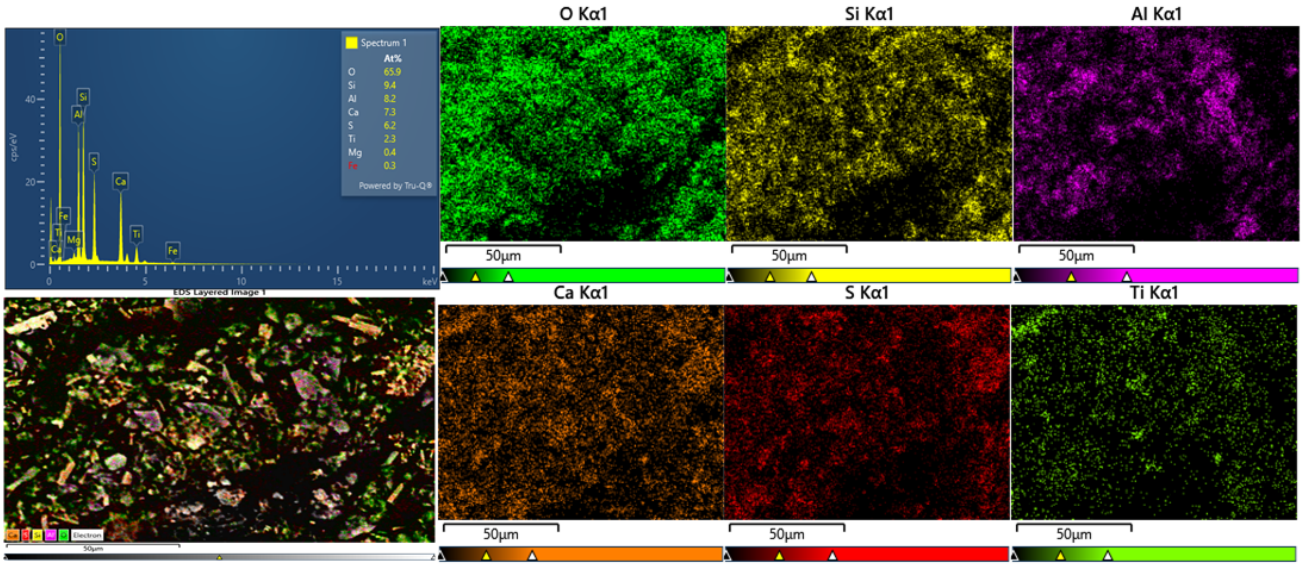

Figure 7. SEM-EDS analysis for Experiment 2.

The SEM coupled with EDS analysis provides insights into the elemental composition of the slag after leaching under 6 bars of oxygen pressure, 150 °C, and a reaction time of 120 min. Due to the localized nature of EDS, the results represent the micro-area component distribution rather than a comprehensive view of the entire sample's bulk composition. This micro-scale analysis can vary due to inherent randomness in the small-area scanning, which may not perfectly correspond to the overall leaching efficiency observed in the bulk material.

The EDS results indicated a high oxygen content of 65.9%, suggesting the presence of oxidized compounds in the analyzed areas of the residual slag. Silicon (Si) was detected at 9.4%, likely pointing to the persistence of silicate minerals that were not fully dissolved

during leaching. Analysis in Figure 7 shows the presence of sulfur (S), which was found at 6.2%, likely as sulfates formed during leaching.

Aluminum (Al) content was found to be 8.2%, while calcium (Ca) and sulfur (S) were present at 7.3% and 6.2%, respectively. These elements suggest the formation of stable compounds such as sulfates that remain in the residual material. Titanium (Ti) and iron (Fe) contents were relatively low, at 2.3% and 0.3%, respectively, which is consistent with the high leaching efficiency of these metals observed in Experiment 2.

The distribution of elements, such as Si and Al, which remain in significant quantities, may reflect the partial dissolution of these components rather than complete removal. The granular and porous morphology observed in the residue suggests selective dissolution, where more soluble components have been removed, leaving less soluble phases intact. The rough and irregular surface features, characteristic of acid leaching, combined with the presence of particles of different sizes, reflect varying degrees of dissolution within the material.

In Figure 8, SEM-EDS results for Tionite S are shown.

The SEM coupled with EDS analysis for Tionite S after leaching under the conditions of 6 bars of oxygen pressure, 180 °C, and a reaction time of 120 min provides valuable micro-scale insights into the composition of the residual slag. It is important to note that EDS analysis reflects the elemental composition of specific micro-areas, and inherent variability in these localized results may not directly correspond to the bulk leaching efficiency observed in macro-scale experiments like in the previous case.

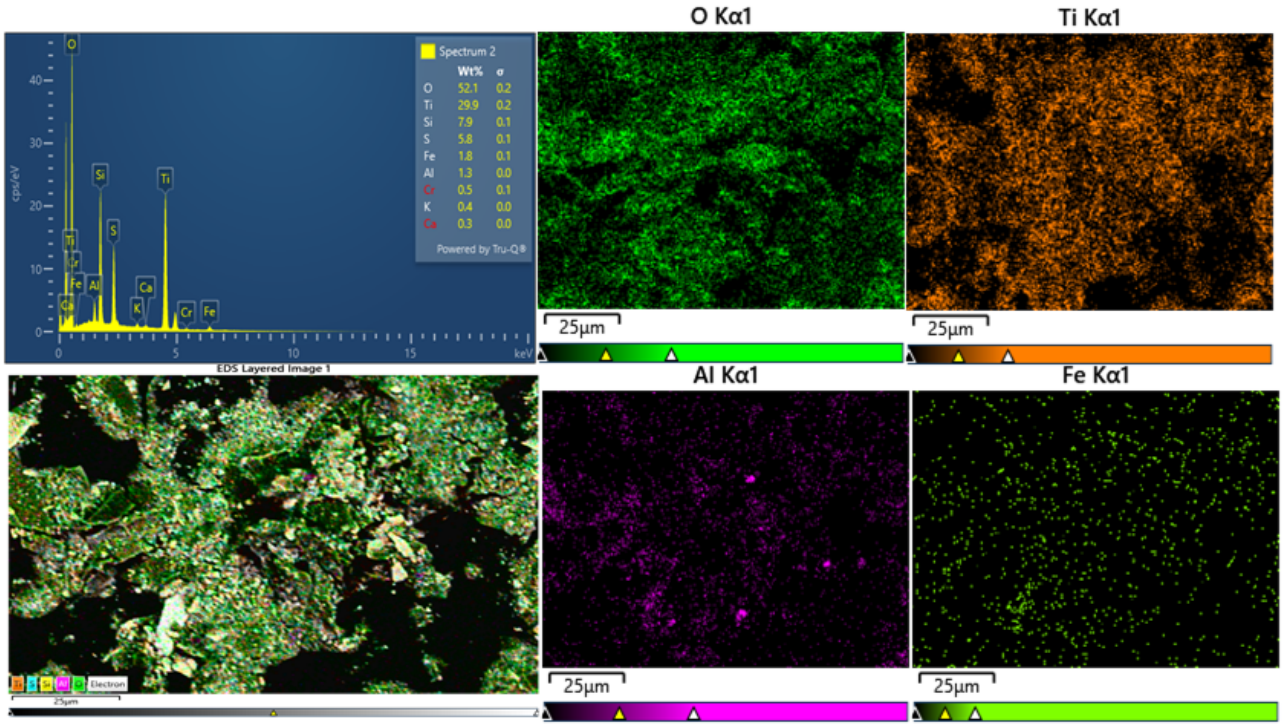

Figure 8. SEM-EDS analysis for Experiment 6.

The EDS results indicate a significant oxygen content of 52.1%, suggesting the presence of oxidized compounds within the specific areas analyzed. Titanium (Ti) appears as the most prominent element after oxygen, with a concentration of 29.9%. This relatively high residual Ti content suggests that under the higher temperature conditions used in this experiment, more stable and less soluble titanium compounds may have formed, which resisted dissolution. However, this micro-scale observation may not fully represent the overall efficiency of titanium leaching across the entire sample.

Silicon (Si) was found at 7.9%, indicating that silicate minerals were not entirely dissolved in the localized areas. Aluminum (Al) was observed at a low concentration of

1.3%, consistent with the generally low leaching efficiency for Al under these conditions, though results may vary throughout the bulk material. Calcium (Ca) was minimal, detected at 0.3%, suggesting only trace amounts in the residue.

Sulfur (S) was detected at 8.8%, likely indicating sulfur-containing compounds, such as sulfates, persisting in the analyzed regions of the slag. Iron (Fe) content was also low at 1.8%, reflecting effective Fe leaching.

The morphology of the residue shows signs of significant structural breakdown, with residual components displaying dissolution and acid leaching effects. The fragmented, porous, and irregular surface likely results from the removal of more soluble phases, leaving behind porous residue typical of acid leaching. This surface structure, which has been observed in the localized areas, aligns with the dissolution patterns of more soluble components, though it may not uniformly represent the material's macro-scale dissolution behavior.

Along with SEM-EDS analysis, XRD analysis of solid residues is also performed (Figure 9).

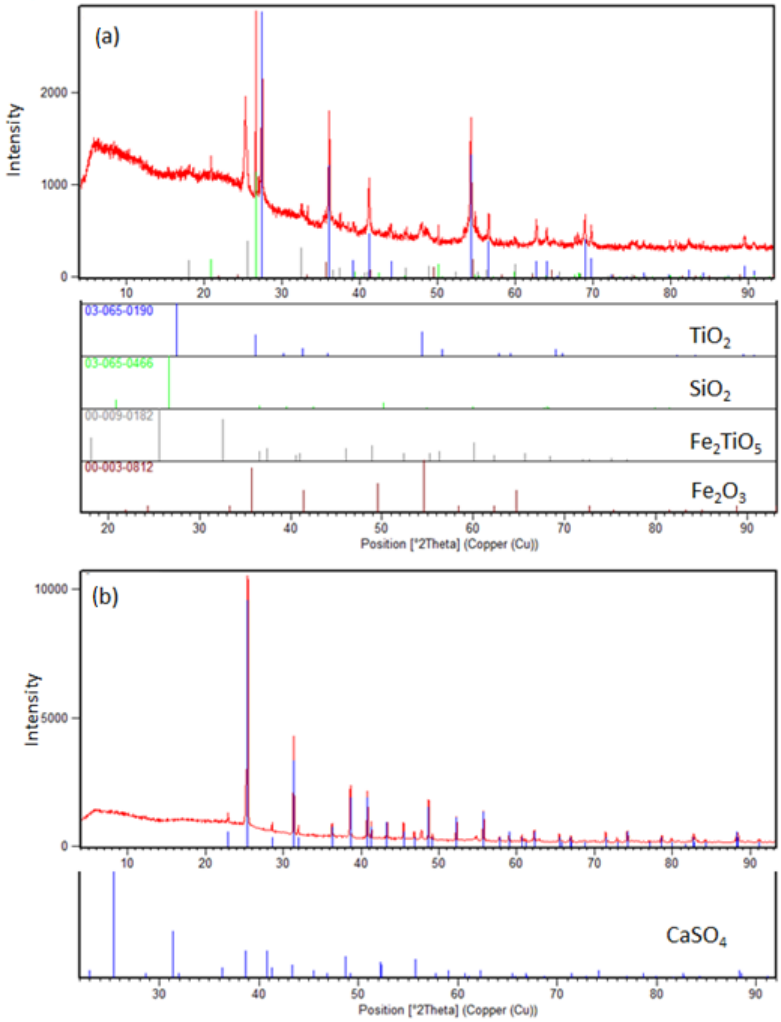

Figure 9. XRD analysis of (**a**) solid residue after Tionite S leaching and (**b**) solid residue after slag leaching.

In the XRD pattern shown in Figure 9a, which corresponds to Tionite S, the peaks are dominated by titanium oxides (TiO_2) and iron-titanium oxides (Fe_2TiO_5), indicating that these phases remain largely unaltered after the leaching process. The presence of these crystalline phases suggests that titanium was not effectively leached, which is consistent with the earlier SEM-EDS analysis that showed a high residual Ti content in the sample.

The detection of iron oxides further supports the SEM-EDS findings, indicating incomplete iron leaching under the tested conditions.

Figure 9b represents the XRD pattern of the slag after leaching. The dominant phase observed is calcium sulfate ($CaSO_4$), implying that most other components, particularly Fe, Ti, and Al, were successfully leached. The absence of significant peaks corresponding to other oxides suggests that the leaching process was effective in dissolving the majority of the original minerals. However, the presence of Si and Al compounds detected in the SEM-EDS results indicates that some of these elements may remain in amorphous forms, which are not visible in the XRD analysis. This difference in crystallinity could explain why these compounds were not detected by XRD despite their presence in the residual material.

In conclusion, the XRD and SEM-EDS results together confirm the limited success of titanium leaching from Tionite S, likely due to its more resistant structure, while the slag exhibited a more complete leaching process, with the residual phase primarily consisting of calcium sulfate. The absence of crystalline Si and Al phases in the XRD pattern of the slag suggests that these elements, although present, are in an amorphous form after leaching.

4. Conclusions

The leaching experiments conducted on both Tionite S and slag using 5 M sulfuric acid under varying conditions of temperature, oxygen pressure, and reaction time offer valuable insights into the effectiveness of the leaching process for extracting iron (Fe), titanium (Ti), and aluminum (Al). The results highlight significant differences in the leaching behaviors of these two materials, which can be attributed to their distinct mineralogical properties and thermal histories.

For the slag, high leaching efficiencies were achieved across all experiments, with near-complete extraction of Fe, Ti, and Al under optimal conditions, especially with increased oxygen pressure. SEM-EDS and XRD analyses confirmed that the residual slag contained minimal Fe and Ti, supporting the high leaching efficiency observed. The slag's structure, formed through carbothermal reduction, appears to be more amenable to leaching due to its altered mineral phases and the breakdown of its crystalline structure during the reduction process, which likely enhanced the dissolution of metals.

In contrast, Tionite S, which has not undergone thermal treatment, exhibited more resistance to leaching. While Fe leaching improved significantly at higher temperatures, Ti remained largely in the residue, as confirmed by the SEM-EDS and XRD results. The high residual Ti content in Tionite S suggests that the natural structure of the mineral is more robust, with titanium potentially existing in forms that are less reactive or more resistant to dissolution under the tested conditions.

The key difference between Tionite S and slag lies in the fact that the slag underwent carbothermal reduction, altering its mineralogical structure and potentially increasing its susceptibility to acid leaching. In contrast, the unaltered natural structure of Tionite S appears to make it more stable and resistant to dissolution, particularly for titanium compounds. This difference in leaching behavior underscores the importance of thermal treatment in enhancing the leachability of certain minerals.

However, further investigation is required to determine whether thermal treatment and reduction would similarly enhance the leaching efficiency of Tionite S. Exploring alternative or additional processing methods, such as further thermal exposure or different leaching agents, could optimize the extraction of valuable elements from Tionite S. Additionally, future studies will incorporate kinetic analyses to provide a deeper understanding of the leaching processes and to optimize conditions for maximum efficiency. This study provides a foundation for improving metal recovery from complex ores and highlights the potential for more efficient processing techniques to extract useful materials from both Tionite S and slag.

Author Contributions: Conceptualization, S.S. and D.K.; methodology, S.S.; software, E.E.-K. and E.U.; validation, S.S., D.K., and S.G.; formal analysis, E.U. and A.M.; investigation, E.U., M.P., and D.K.; resources, S.S.; data curation, S.S. and A.M; writing—original draft preparation, D.K. and S.S.;

writing—review and editing, S.G., M.P., and E.E.-K.; visualization, D.K.; supervision, B.F. and M.P.; project administration, S.S.; funding acquisition, S.S. and M.P. All authors have read and agreed to the published version of the manuscript.

Funding: This research was funded by the European Commission, grant number 101135077 (EURO-TITAN project).

Data Availability Statement: Data are contained within the article.

Conflicts of Interest: The authors declare no conflicts of interest.

References

1. Gázquez, M.J.; Bolívar, J.P.; García-Tenorio García-Balmaseda, R.; Vaca, F. A Review of the Production Cycle of Titanium Dioxide Pigment. *Mater. Sci. Appl.* **2014**, *5*, 441–458. [CrossRef]
2. Sadeghi, M.H.; Nasr Esfahany, M. Development of a Safe and Environmentally Friendly Sulfate Process for the Production of Titanium Oxide. *Ind. Eng. Chem. Res.* **2022**, *61*, 1786–1796. [CrossRef]
3. How to Manufacture Titanium Dioxide by Chloride Process. Available online: https://www.fangyuan-tio2.com/how-to-manufacture-titanium-dioxide-by-chloride-process.html (accessed on 29 July 2024).
4. Braun, J.H.; Baidins, A.; Marganski, R.E. TiO_2 Pigment Technology: A Review. *Prog. Org. Coat.* **1992**, *20*, 105–138. [CrossRef]
5. Filippou, D.; Hudon, G. Iron Removal and Recovery in the Titanium Dioxide Feedstock and Pigment Industries. *JOM* **2009**, *61*, 36–42. [CrossRef]
6. Meng, F.; Xue, T.; Liu, Y.; Wang, W.; Qi, T. Treatment of Tionite Residue from Titanium Oxide Industry for Recovery of TiO_2 and Removal of Silica. *Hydrometallurgy* **2016**, *161*, 112–116. [CrossRef]
7. Chen, D.B. *Practical Questions and Answers in the Production of Titanium Doxide from Sulfate Process*; Chemical Industry Press: Beijing, China, 2009.
8. Hajjaji, W.; Costa, G.; Zanelli, C.; Ribeiro, M.J.; Seabra, M.P.; Dondi, M.; Labrincha, J.A. An Overview of Using Solid Wastes for Pigment Industry. *J. Eur. Ceram. Soc.* **2012**, *32*, 753–764. [CrossRef]
9. Labrincha, J.A.; Marques, J.I.; Hajjaji, W.; Senff, L.; Zanelli, C.; Dondi, M.; Rocha, F. Novel Inorganic Products Based on Industrial Wastes. *Waste Biomass Valori.* **2014**, *5*, 385–392. [CrossRef]
10. Archambo, M.S.; Kawatra, S.K. Utilization of Bauxite Residue: Recovering Iron Values Using the Iron Nugget Process. *Miner. Process. Extr. Metall. Rev.* **2021**, *42*, 222–230. [CrossRef]
11. Liu, Y.; Naidu, R. Hidden Values in Bauxite Residue (Red Mud): Recovery of Metals. *Waste Manag.* **2014**, *34*, 2662–2673. [CrossRef] [PubMed]
12. Qi, Y. The Neutralization and Recycling of Red Mud-a Review. *J. Phys. Conf. Ser.* **2021**, *1759*, 12004. [CrossRef]
13. Winkler, D.; Bidló, A.; Bolodár-Varga, B.; Erdő, Á.; Horváth, A. Long-Term Ecological Effects of the Red Mud Disaster in Hungary: Regeneration of Red Mud Flooded Areas in a Contaminated Industrial Region. *Sci. Total. Environ.* **2018**, *644*, 1292–1303. [CrossRef] [PubMed]
14. Environmental and Radiation Concerns of Red Mud. Available online: http://large.stanford.edu/courses/2018/ph241/pontius1/ (accessed on 20 July 2024).
15. Amritphale, S.S.; Anshul, A.; Chandra, N.; Ramakrishnan, N. A Novel Process for Making Radiopaque Materials Using Bauxite—Red Mud. *J. Eur. Ceram. Soc.* **2007**, *27*, 1945–1951. [CrossRef]
16. Liu, W.; Yang, J.; Xiao, B. Application of Bayer Red Mud for Iron Recovery and Building Material Production from Alumosilicate Residues. *J. Hazard. Mater.* **2009**, *161*, 474–478. [CrossRef] [PubMed]
17. Pérez-Villarejo, L.; Corpas-Iglesias, F.A.; Martínez-Martínez, S.; Artiaga, R.; Pascual-Cosp, J. Manufacturing New Ceramic Materials from Clay and Red Mud Derived from the Aluminium Industry. *Constr. Build. Mater.* **2012**, *35*, 656–665. [CrossRef]
18. Faraji, F.; Alizadeh, A.; Rashchi, F.; Mostoufi, N. Kinetics of Leaching: A Review. *Rev. Chem. Eng.* **2022**, *38*, 113–148. [CrossRef]
19. Free, M.L. *Hydrometallurgy: Fundamentals and Applications*; Springer Nature: Berlin, Germany, 2021. [CrossRef]
20. Othusitse, N.; Muzenda, E. Predictive Models of Leaching Processes: A Critical Review. In Proceedings of the 7th International Conference on Latest Trends in Engineering & Technology (ICLTET'2015), Pritoria, South Africa, 26–27 November 2015. [CrossRef]
21. Zhou, K.; Teng, C.; Zhang, X.; Peng, C.; Chen, W. Enhanced Selective Leaching of Scandium from Red Mud. *Hydrometallurgy* **2018**, *182*, 57–63. [CrossRef]
22. Borra, C.R.; Mermans, J.; Blanpain, B.; Pontikes, Y.; Binnemans, K.; Van Gerven, T. Selective Recovery of Rare Earths from Bauxite Residue by Combination of Sulfation, Roasting and Leaching. *Min. Eng.* **2016**, *92*, 151–159. [CrossRef]